LETTERS

The RNA-binding protein KSRP promotes the biogenesis of a subset of microRNAs

Michele Trabucchi[1], Paola Briata[2]*, MariaFlor Garcia-Mayoral[3], Astrid D. Haase[4], Witold Filipowicz[4], Andres Ramos[3], Roberto Gherzi[2]* & Michael G. Rosenfeld[1]*

Consistent with the role of microRNAs (miRNAs) in down-regulating gene expression by reducing the translation and/or stability of target messenger RNAs[1], the levels of specific miRNAs are important for correct embryonic development and have been linked to several forms of cancer[2–4]. However, the regulatory mechanisms by which primary miRNAs (pri-miRNAs) are processed first to precursor miRNAs (pre-miRNAs) and then to mature miRNAs by the multiprotein Drosha and Dicer complexes[5–8], respectively, remain largely unknown. The KH-type splicing regulatory protein (KSRP, also known as KHSRP) interacts with single-strand AU-rich-element-containing mRNAs and is a key mediator of mRNA decay[9,10]. Here we show in mammalian cells that KSRP also serves as a component of both Drosha and Dicer complexes and regulates the biogenesis of a subset of miRNAs. KSRP binds with high affinity to the terminal loop of the target miRNA precursors and promotes their maturation. This mechanism is required for specific changes in target mRNA expression that affect specific biological programs, including proliferation, apoptosis and differentiation. These findings reveal an unexpected mechanism that links KSRP to the machinery regulating maturation of a cohort of miRNAs that, in addition to its role in promoting mRNA decay, independently serves to integrate specific regulatory programs of protein expression.

We analysed the immunopurified Dicer-containing complex[11] by mass spectroscopy and identified, amongst other proteins, KSRP (Supplementary Fig. 1a)—a highly conserved nucleo-cytoplasmic RNA-binding protein regulating distinct steps of mRNA life cycle[12,13] (Supplementary Fig. 1b–d). KH domains 3 and 4 of KSRP (KH3–4) are required to promote AU-rich element (ARE)-containing labile mRNA decay[9,10]. Coimmunoprecipitation revealed that KSRP is an integral component of the Dicer complex in HeLa cells (Fig. 1a). On *Dicer*-knockdown-induced (Supplementary Fig. 2a) pre-miRNA upregulation, an anti-KSRP antibody immunoprecipitated *pre-let-7a*[14] (Fig. 1b). Recombinant KSRP directly interacted with *pre-let-7a-1*, and KH3–4 accounted for the high-affinity binding to RNA (Supplementary Fig. 3a). KSRP interacted with the terminal loop (TL) of *pre-let-7a-1* (*TL-let-7a-1*) but did not associate with either single- or double-stranded mature let-7a (Fig. 1c), with KH3–4 accounting for KSRP binding to *TL-let-7a-1* (Supplementary Fig. 3b).

We titrated the protein with increasing amounts of *TL-let-7a-1*, and *TL-let-7a-1* with increasing amount of protein, while monitoring the binding by NMR and circular dichroism, respectively. KH3–4 binds to *TL-let-7a-1* with a 1:1 stoichiometry and a dissociation constant (K_d) of ~50 nM (Supplementary Fig. 3c) whereas single KH3 and KH4 domains bind to *TL-let-7a-1* with a K_d of ~500 nM and ~40 μM, respectively (Supplementary Fig. 3d, e). In contrast to

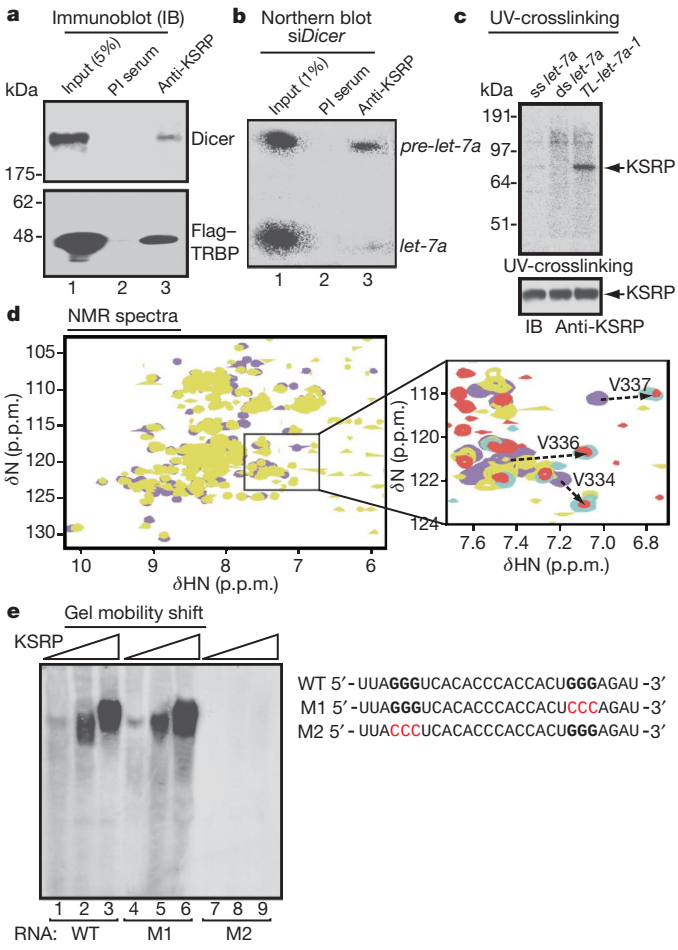

Figure 1 | KSRP, a component of Dicer complex, interacts with the TL of *pre-let-7a-1*. **a**, Coimmunoprecipitation of endogenous KSRP and either Dicer or Flag–TRBP in HeLa cell extracts. PI serum, preimmune serum. **b**, Coimmunoprecipitation of KSRP and *pre-let-7a* in HeLa cells transiently transfected with *Dicer* small interfering RNA (si*Dicer*). **c**, KSRP (300 nM) binds to *TL-let-7a-1* but not to single-stranded (ss) or double-stranded (ds) *let-7a*. UV, ultraviolet. **d**, Superimposition of ^{15}N-^{1}H HSQC spectra of KH3–4-free (violet) and bound to *TL-let-7a-1* (yellow). In the magnified panel, spectra of bound KH3 (cyan) and KH2-3 (red) are also shown. Arrows highlight the shift of a few representative peaks in the core of the RNA-binding groove. **e**, Interaction of KSRP (50–300 nM) with either wild-type (WT) *TL-let-7a-1* or two distinct mutants (M1 and M2). Bold indicates G stretches and red indicates mutations.

[1]Howard Hughes Medical Institute, Department and School of Medicine, University of California, San Diego, 9500 Gilman Drive, Room 345, La Jolla, California 92093-0648, USA. [2]Istituto Nazionale per la Ricerca sul Cancro (IST), Largo R. Benzi, 10; 16132 Genova, Italy. [3]Division of Molecular Structure, National Institute for Medical Research, The Ridgeway, Mill Hill, London NW7 1AA, UK. [4]Friedrich Miescher Institute for Biomedical Research, PO Box 2543, 4002 Basel, Switzerland.
*These authors contributed equally to this work.

what was observed in the KH3–TNF-α ARE interaction[10], KH3 recognizes a specific site in the *TL-let-7a-1* and contributes most of the binding affinity in the KH3–4–RNA interaction, whereas KH4 has an auxiliary role. Comparison of the chemical shift changes undergone by KH3 amide resonances upon RNA binding in the isolated KH3 and within the two-domain KH2–3 and KH3–4 constructs showed that the bound position of the resonance affected by *TL-let-7a-1* binding is the same whether or not KH2 or KH4 is present (Fig. 1d and Supplementary Fig. 3f). NMR spectra showed that the position of nearly all of the resonances of the RNA-bound KH3 is the same for the *TL-let-7a-1* and the entire *pre-let-7a-1* (Supplementary Fig. 3g).

Our recent work indicated that KH3 recognizes short G-rich stretches with high specificity and affinity[15]. The *TL-let-7a-1* presents two GGG triplets, supporting the idea that KH3 docks KSRP on a specific site and that KSRP–*pre-let-7a-1* recognition takes place using a very different mode and a considerably higher affinity compared with ARE mRNA targets[10,16]. Mutational analysis of *TL-let-7a-1* revealed that the 5′ GGG triplet accounts for high-affinity binding to KSRP (Fig. 1e).

KSRP knockdown in both HeLa and NIH-3T3 cells (Supplementary Fig. 2b, c) abrogated the endogenous let-7a-mediated post-transcriptional silencing of a reporter construct containing six let-7a binding sites (let-7a6×BS) (Fig. 2a). *KSRP* knockdown inhibited the effect of both transfected *pri-* and *pre-let-7a-1* on let-7a6×BS reporter but left transfected mature let-7a function unaffected (Fig. 2b and Supplementary Fig. 4a, b). Control *HNRNPD* (previously known as *AUF1*) knockdown (Supplementary Fig. 2d) had no effect (Fig. 2a, b).

Recombinant KSRP increased the processing activity of Dicer (Fig. 2c) whereas KSRP immunodepletion from 293T extracts (Supplementary Fig. 2e) removed the *pre-let-7a-1* processing activity (Supplementary Fig. 4c) leaving mature let-7a unaffected (Supplementary Fig. 4d). Finally, immunopurified KSRP-containing complexes specifically processed *pre-let-7a-1* into mature let-7a (Supplementary Fig. 4e–g).

To investigate whether all pre-miRNAs are regulated by KSRP, we performed miRNA microarray analysis. Transient *KSRP* knockdown in HeLa cells significantly reduced (>1.5-fold) the expression of 14 miRNAs (Supplementary Fig. 5a) and reduced by 1.2–1.5-fold the expression of 20 additional miRNAs (Supplementary Table 1). Northern blot analysis in both HeLa and NIH-3T3 cells confirmed that let-7a, miR-26b, miR-20, miR-106a, miR-21 and miR-16 were reduced by 40–70% upon *KSRP* knockdown whereas miR-23b and miR-24 were unaffected (Fig. 2d, Supplementary Fig. 5b–e and data not shown). Ultraviolet crosslinking and *in vitro* processing experiments showed the selectivity of KSRP binding and KSRP-induced

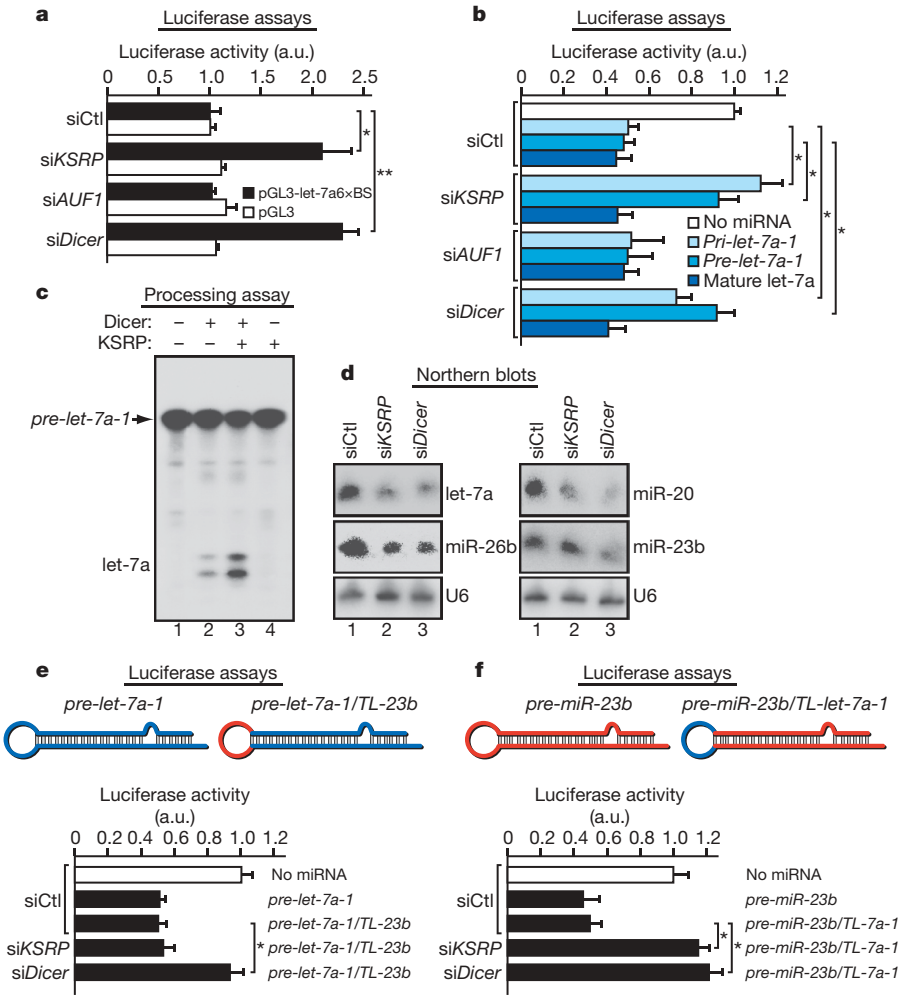

Figure 2 | KSRP regulates *pre-let-7a-1* processing and controls the expression of certain miRNAs. **a**, *KSRP* knockdown reduces the effect of endogenous let-7a on the activity of pGL3-let-7a6×BS. Student's *t*-test: $*P < 0.05$, $**P < 0.01$. a.u., arbitrary units; siCtl, control siRNA. **b**, *KSRP* knockdown reduces the effect of either *pri-let-7a-1* or *pre-let-7a-1*, but not of mature let-7a, on pGL3-let-7a6×BS activity. $*P < 0.05$. **c**, Recombinant KSRP increases the processing activity of recombinant Dicer on *pre-let-7a*. **d**, Analysis of total RNA from control, *KSRP*- or *Dicer*-knockdown HeLa cells. **e**, **f**, *KSRP* knockdown does not reduce the effect of a chimaeric *pre-let-7a-1*, comprising the TL of *pre-miR-23b*, on the activity of pGL3-let-7a6×BS (**e**) but impairs the effect of a chimaeric *pre-miR-23b*, comprising the TL of *pre-let-7a-1*, on the activity of pGL3-miR-23b3×BS (**f**). $*P < 0.05$. All data are presented as mean and s.d. ($n = 4$).

processing for those miRNAs for which expression was regulated by KSRP (Supplementary Fig. 6a–c and data not shown). Interestingly, the *TL-miR-21* does not contain any GGG triplets but displays two potential non-optimal binding sites for KSRP KH3 and KH4 (Supplementary Fig. 6d and ref. 15). Mutation of the two G residues in the GUUG 5′ element abrogated the KSRP interaction whereas mutation of the 3′ GG doublet only reduced the binding affinity (Supplementary Fig. 6d).

To investigate the function of TL–KSRP interaction, we used chimaeric pre-miRNAs with swapped loop sequences. *KSRP* knockdown did not affect the expression of a reporter containing let-7a-binding sites when a chimaeric *pre-let-7a-1* comprising the TL of miR-23b was expressed in HeLa cells (Fig. 2e). Conversely, expression of a reporter containing miR-23b-binding sites was impaired by *KSRP* knockdown in HeLa cells expressing a chimaeric *pre-miR-23b* containing the TL of let-7a-1 (Fig. 2f and Supplementary Fig. 6e).

Because pre-miRNA accumulation induced by *KSRP* knockdown was low in comparison to that induced by *Dicer* knockdown (Supplementary Fig. 7a), and *KSRP* knockdown increased the levels of *pri-let-7a-1* and *pri-miR-21* (Supplementary Fig. 7b), we hypothesized an involvement of KSRP in pri-miRNA processing. KSRP coimmunoprecipitated with Flag-tagged Drosha and DGCR8 (Fig. 3a), and anti-KSRP antibody immunoprecipitated *pri-let-7a-1* and *pri-miR-21* but not *pri-miR23b*, *pri-miR-24* and *pri-miR-17* (Fig. 3b and Supplementary Fig. 7c). Endogenous, transfected and recombinant KSRP specifically interacted with *pri-let-7a-1* (Supplementary Fig. 8a–c). Immunopurified KSRP-containing complexes processed *pri-let-7a-1* similarly to Drosha-containing immunopurified complexes (Supplementary Fig. 9a). Either stable or transient *KSRP* knockdown in 293T, HeLa and NIH-3T3 cells reduced the *pri-let-7a-1* processing (Supplementary Fig. 9b–d) leaving the processing of *pri-miR-23b* unaffected (Supplementary Fig. 9b, right panel, and data not shown). Addition of recombinant KSRP to 293T cells stably transfected with short hairpin RNA to *KSRP* (293T sh*KSRP*) extracts restored *pri-let-7a-1* processing whereas KSRP overexpression in 293T cells strongly increased *pri-let-7a-1* processing (Fig. 3c and Supplementary Fig. 9e).

We explored the possibility that KSRP favours the association of enzymatic complexes with certain miRNA precursors. Indeed, *KSRP* knockdown abrogated the interaction of Drosha with *pri-let-7a-1* and *pri-miR-21* (Fig. 3d) and strongly reduced the binding of Dicer to *pre-let-7a-1* and *pre-miR-21* (Fig. 3e). In contrast, *KSRP* knockdown did not affect the interaction of the same pri-miRNAs and pre-miRNAs with either DGCR8 or TARBP2P (also known as TRBP; Supplementary Fig. 10a and data not shown)[5,11].

KSRP knockdown increased mRNA levels of two let-7 targets, NRAS and MYC[17,18] (Supplementary Fig. 10b), and specificity was established because cotransfection of mature let-7a abolished this effect (Supplementary Fig. 10c, d). Furthermore, *KSRP* knockdown in U2OS osteosarcoma cells reduced the expression of mature let-7a, significantly upregulated cell proliferation[19] (Fig. 4a and data not shown) and reduced the anti-proliferative effect of transfected *pri-let-7a-1* but not of mature let-7a (Fig. 4a and Supplementary Fig. 11a). Similarly, *KSRP* knockdown prevented *pri-miR-16-1*-induced apoptosis[20] but did not affect the activity of transfected mature miR-16 (Supplementary Fig. 11b, c). Recently, an essential role of certain miRNAs (miR-1, miR-133a and miR-206) in C2C12 myoblast differentiation has been reported[21,22]. *KSRP* knockdown in C2C12 reduced the maturation of 'myogenic' miRNAs (Supplementary Fig. 12a–c). The interaction of KSRP with *pri-miR-206*, *pri-miR-1-1* and *pri-miR-1-2* was increased by pro-differentiative stimuli (differentiation medium, Supplementary Fig. 12d). Finally, *KSRP* knockdown inhibited the miR-206-induced downregulation of direct target mRNAs, including those encoding gap junction protein α1

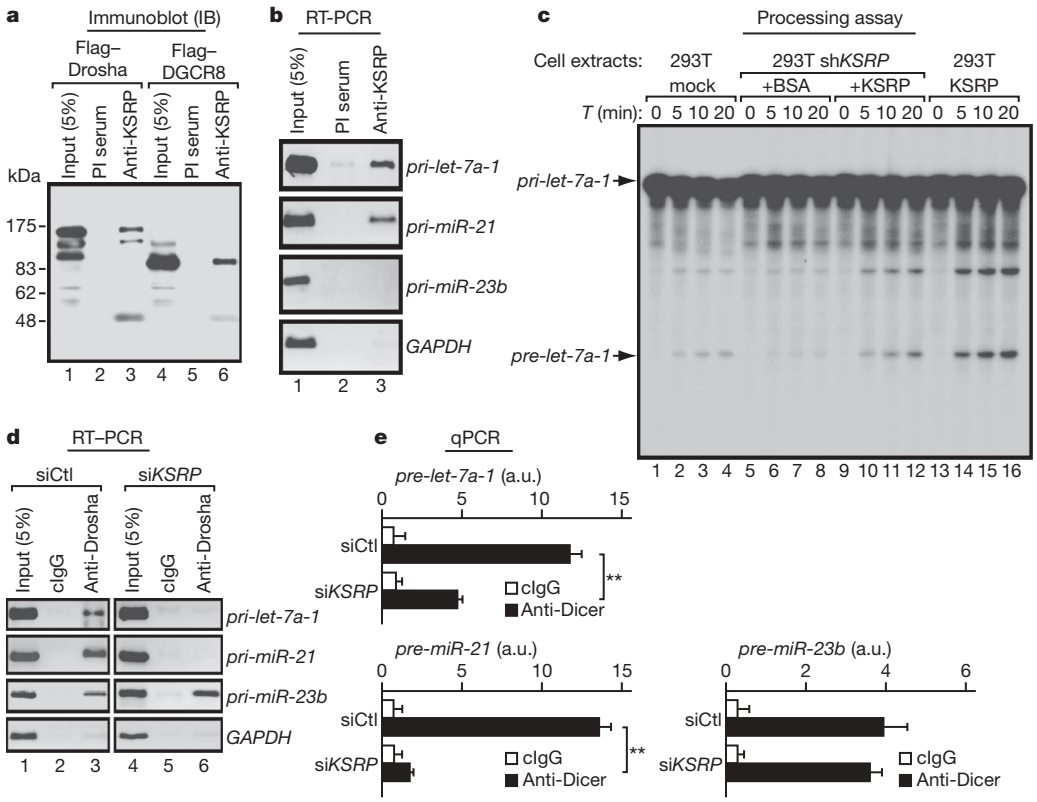

Figure 3 | KSRP is a component of the microprocessor complex, interacts with *pri-let-7a-1* favouring its processing, and is required for interaction of both Drosha and Dicer complexes with let-7a precursors.
a, Coimmunoprecipitation of endogenous KSRP with either Flag–Drosha or Flag–DGCR8. **b**, Anti-KSRP immunoprecipitates select pri-miRNAs. *GAPDH*, glyceraldehyde-3-phosphate dehydrogenase. **c**, KSRP (50 nM) restores *pri-let-7a-1* processing when added to extracts from sh*KSRP* stably transfected cells whereas KSRP overexpression enhances *pri-let-7a-1* processing. **d**, **e**, *KSRP* knockdown impairs the interaction of Drosha and Dicer with certain miRNA precursors. $^{**}P < 0.01$. All data are presented as mean and s.d. ($n = 4$). cIgG, control immunoglobulin G.

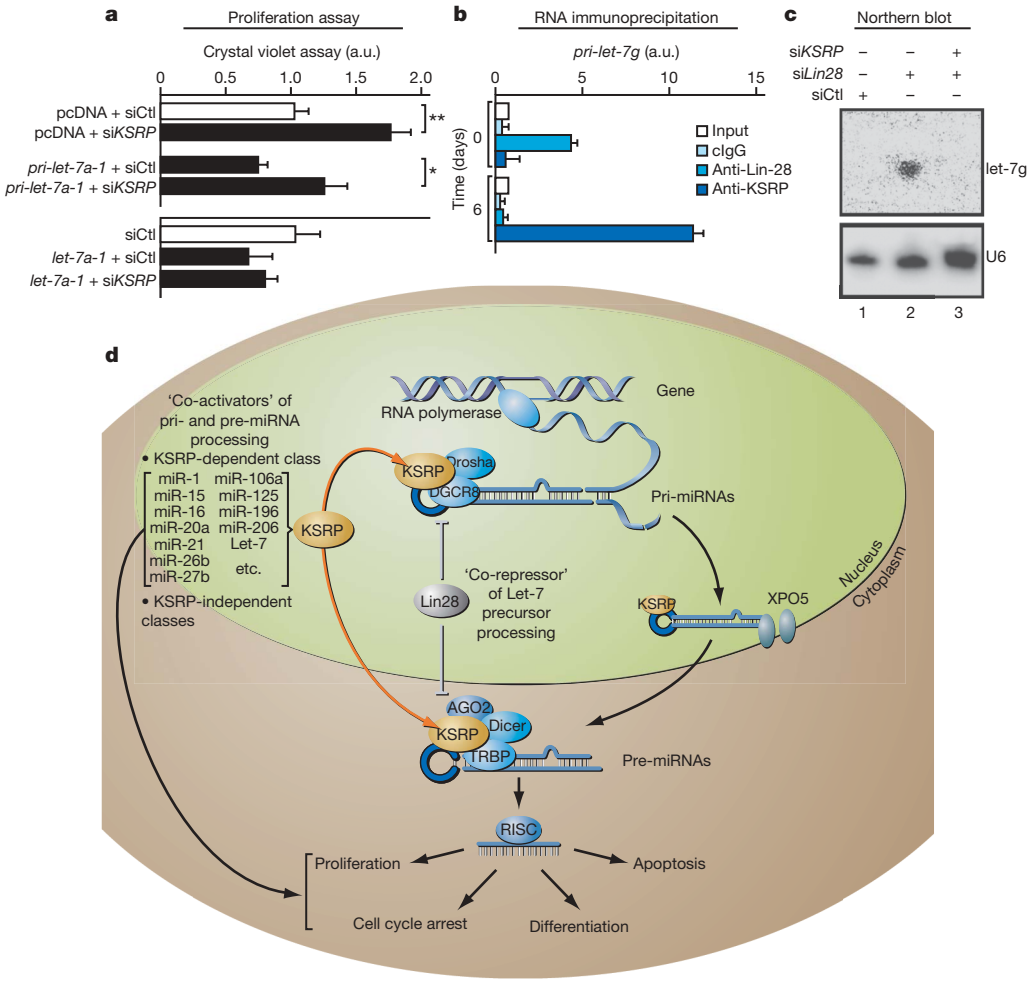

Figure 4 | KSRP affects let-7-regulated cell proliferation and is involved in Lin28-regulated maturation of let-7g in P19 cells. **a**, *KSRP* knockdown increases proliferation and inhibits the antiproliferative effect of transfected *pri-let-7a-1* but not of mature let-7a in U2OS cells. $*P < 0.05$, $**P < 0.01$. **b**, KSRP interacts with *pri-let-7g* only in differentiated P19 cells. **c**, *Lin28* knockdown in undifferentiated P19 cells induces the expression of let-7g. Concomitant Lin28 and KSRP knockdown abolishes let-7g expression. **d**, A model for KSRP-dependent regulation of processing of certain miRNAs. All data are presented as mean and s.d. ($n = 4$).

(also known as connexin 43) and DNA pol α[22], impairing C2C12 differentiation (Supplementary Fig. 12e, f).

Recently, four papers[8,23–25] demonstrated that the maturation of let-7 is blocked by Lin28 in undifferentiated embryonic stem cells and P19 cells. We observed that KSRP interacts with *pri-let-7g* in P19 cells upon retinoic-acid-induced differentiation (Fig. 4b). *Lin28* knockdown in undifferentiated P19 cells induced let-7g expression whereas concomitant *KSRP* knockdown abolished this effect (Fig. 4c) indicating that, upon *Lin28* knockdown, KSRP promotes maturation of let-7g precursors. Similarly, upon P19 differentiation, Lin28 expression is abrogated[8,23–25], thus allowing KSRP to promote processing of let-7g precursors. This is also compatible with the recently reported mechanism of action of Lin28 (ref. 26). We suggest that TL is a pivotal structure where miRNA processing 'activators' (for example, KSRP) as well as 'repressors' (for example, Lin28) function in a coordinated way to convey proliferating, apoptotic or differentiating cues into changes of miRNA expression (Fig. 4d).

In conclusion, KSRP is a key regulator of the processing of a sizeable subset of miRNA precursors on the basis of its high-affinity binding to their TL. The TLs of most KSRP-regulated microRNAs (let-7-a, -b, -c, -d, -f, -i and miR-196a) contain short G-rich stretches of at least three Gs that represent the optimal binding site for KH3 (ref. 15). However, the TLs of the other KSRP target miRNAs contain instead two sequential or isolated Gs and our data on the KSRP–TL-miR-21 interaction show that a significant, albeit different, contribution to the binding is provided by both G-containing stretches (Supplementary Fig. 6d). These data underscore the adaptability of the protein to a broad range of single-stranded RNA sequences[15,16].

Upon binding, KSRP could optimize the positioning and/or recruitment of both the miRNA precursor processing complexes through protein–protein interactions (Supplementary Fig. 13a–c). The RNase sensitivity of KSRP–exportin-5 (XPO5) interaction indicates that KSRP is associated with the TL of target miRNA precursors during nucleo-cytoplasmic transit (Supplementary Fig. 13a). Sequential immunoprecipitation experiments indicate that at least two pools of miRNA precursors exist, one associated with processing complexes including KSRP and the other associated with processing complexes that do not include KSRP (Supplementary Fig. 14). For example, it has been reported[27] that HNRNPA1 binds to the TL of miRNAs for which processing is not affected by KSRP.

Altogether, our findings uncover an additional level of complexity for miRNA-dependent regulation of gene expression that contributes to the modulation of different biological programs.

METHODS SUMMARY

Immunoprecipitation of ribonucleoprotein complexes was performed as described previously[28] with minor modifications. In brief, cells lysates were immunoprecipitated with either protein A- or protein A/protein G–Sepharose-coupled antibodies at 4 °C overnight (16 h). Pellets were sequentially washed with the following buffers: buffer I (0.1% SDS, 1% Triton X-100, 2 mM EDTA, 20 mM Tris-HCl, pH 8.1, 150 mM NaCl); buffer II (0.1% SDS, 1% Triton X-100, 2 mM EDTA, 20 mM Tris-HCl, pH 8.1, 500 mM NaCl); and buffer III (0.25 M LiCl, 1%

NP-40, 1% deoxycholate, 1 mM EDTA, 10 mM Tris-HCl, pH 8.1). Total RNA was prepared using Trizol, retrotranscribed using random primers and amplified by PCR. The primer sequences are detailed in Supplementary Table 2.

Full Methods and any associated references are available in the online version of the paper at www.nature.com/nature.

Received 15 January 2008; accepted 25 March 2009.
Published online 20 May 2009.

1. Pillai, R. S., Bhattacharyya, S. N. & Filipowicz, W. Repression of protein synthesis by miRNAs: how many mechanisms? *Trends Cell Biol.* **17,** 118–126 (2007).
2. Kumar, M. S., Lu, J., Mercer, K. L., Golub, T. R. & Jacks, T. Impaired microRNA processing enhances cellular transformation and tumorigenesis. *Nature Genet.* **39,** 673–677 (2007).
3. Thomson, J. M. *et al.* Extensive post-transcriptional regulation of microRNAs and its implications for cancer. *Genes Dev.* **20,** 2202–2207 (2006).
4. Calin, G. A. & Croce, C. M. MicroRNA signatures in human cancers. *Nature Rev. Cancer* **6,** 857–866 (2006).
5. Kim, V. N., Han, J. & Siomi, M. C. Biogenesis of small RNAs in animals. *Nature Rev. Mol. Cell Biol.* **10,** 126–139 (2009).
6. Obernosterer, G., Leuschner, P. J., Alenius, M. & Martinez, J. Post-transcriptional regulation of microRNA expression. *RNA* **12,** 1161–1167 (2006).
7. Guil, S. & Caceres, J. F. The multifunctional RNA-binding protein hnRNP A1 is required for processing of miR-18a. *Nature Struct. Mol. Biol.* **14,** 591–596 (2007).
8. Viswanathan, S. R., Daley, G. Q. & Gregory, R. I. Selective blockade of microRNA processing by Lin28. *Science* **320,** 97–100 (2008).
9. Gherzi, R. *et al.* A KH domain RNA binding protein, KSRP, promotes ARE-directed mRNA turnover by recruiting the degradation machinery. *Mol. Cell* **14,** 571–583 (2004).
10. Garcia-Mayoral, M. F. *et al.* The structure of the C-terminal KH domains of KSRP reveals a noncanonical motif important for mRNA degradation. *Structure* **15,** 485–498 (2007).
11. Haase, A. D. *et al.* TRBP, a regulator of cellular PKR and HIV-1 virus expression, interacts with Dicer and functions in RNA silencing. *EMBO Rep.* **6,** 961–967 (2005).
12. Min, H., Turck, C. W., Nikolic, J. M. & Black, D. L. A new regulatory protein, KSRP, mediates exon inclusion through an intronic splicing enhancer. *Genes Dev.* **11,** 1023–1036 (1997).
13. Kroll, T. T., Zhao, W. M., Jiang, C. & Huber, P. W. A homolog of FBP2/KSRP binds to localized mRNAs in Xenopus oocytes. *Development* **129,** 5609–5619 (2002).
14. Roush, S. & Slack, F. J. The let-7 family of microRNAs. *Trends Cell Biol.* **18,** 505–516 (2008).
15. Garcia-Mayoral, M. F., Diaz-Moreno, I., Hollingworth, D. & Ramos, A. The sequence selectivity of KSRP explains its flexibility in the recognition of the RNA targets. *Nucleic Acids Res.* **36,** 5290–5296 (2008).
16. Ruggiero, T. *et al.* Identification of a set of KSRP target transcripts upregulated by PI3K-AKT signaling. *BMC Mol. Biol.* **8,** 28 (2007).
17. Johnson, S. M. *et al.* RAS is regulated by the let-7 microRNA family. *Cell* **120,** 635–647 (2005).
18. Sampson, V. B. *et al.* MicroRNA let-7a down-regulates MYC and reverts MYC-induced growth in Burkitt lymphoma cells. *Cancer Res.* **67,** 9762–9770 (2007).
19. Lee, Y. S. & Dutta, A. The tumor suppressor microRNA let-7 represses the HMGA2 oncogene. *Genes Dev.* **21,** 1025–1030 (2007).
20. Cimmino, A. *et al.* miR-15 and miR-16 induce apoptosis by targeting BCL2. *Proc. Natl Acad. Sci. USA* **102,** 13944–13949 (2005).
21. Chen, J. F. *et al.* The role of microRNA-1 and microRNA-133 in skeletal muscle proliferation and differentiation. *Nature Genet.* **38,** 228–233 (2006).
22. Kim, H. K., Lee, Y. S., Sivaprasad, U., Malhotra, A. & Dutta, A. Muscle-specific microRNA miR-206 promotes muscle differentiation. *J. Cell Biol.* **174,** 677–687 (2006).
23. Newman, M. A., Thomson, J. M. & Hammond, S. M. Lin-28 interaction with the Let-7 precursor loop mediates regulated microRNA processing. *RNA* **14,** 1539–1549 (2008).
24. Rybak, A. *et al.* A feedback loop comprising lin-28 and let-7 controls pre-let-7 maturation during neural stem-cell commitment. *Nature Cell Biol.* **10,** 987–993 (2008).
25. Piskounova, E. *et al.* Determinants of microRNA processing inhibition by the developmentally regulated RNA-binding protein Lin28. *J. Biol. Chem.* **283,** 21310–21314 (2008).
26. Heo, I. *et al.* Lin28 mediates the terminal uridylation of let-7 precursor microRNA. *Mol. Cell* **32,** 276–284 (2008).
27. Michlewski, G., Guil, S., Semple, C. A. & Caceres, J. F. Posttranscriptional regulation of miRNAs harboring conserved terminal loops. *Mol. Cell* **32,** 383–393 (2008).
28. Chen, C. Y. *et al.* Nucleolin and YB-1 are required for JNK-mediated interleukin-2 mRNA stabilization during T-cell activation. *Genes Dev.* **14,** 1236–1248 (2000).

Supplementary Information is linked to the online version of the paper at www.nature.com/nature.

Acknowledgements We thank V. Narry Kim, T. C. Hobman, I. G. Macara, D. Srivastava and J. G. Belasco for reagents, G. Corte for sharing laboratory facilities and critical reading, Y. T. Liu for use of the microarray facility, M. Ponassi and C. Nelson for technical assistance, I. Diaz-Moreno, M. Doyle, S. Martin and D. Hollingworth for discussions and reagents, and A. Pasquinelli and A. De Flora for comments and discussions. Part of the studies has been conducted in the laboratories and facilities of the Centro Biotecnologie Avanzate (CBA, Genova, Italy). M.G.R. is an investigator with the Howard Hughes Medical Institute. M.T. is supported by a post-doctoral fellowship from the Italian Telethon Foundation. This work has been partly supported by grants from Italian ISS (527B/2B/6), AIRC and CIPE 2007 to R.G., ISS (526D/39) to P.B., the EC FP6 Program Sirocco to W.F. and NIH grants DK018477, DK39949 and HL065445 to M.G.R. P.B. is recipient of a Senior Scholar Consultancy grant from AICF. Structural work on KSRP–RNA interaction is supported by grant WT022088MA from the Wellcome Trust. NMR spectra were recorded at the MRC Biomedical NMR Centre, London. The Friedrich Miescher Institute is supported by the Novartis Research Foundation.

Author Information Reprints and permissions information is available at www.nature.com/reprints. Correspondence and requests for materials should be addressed to M.G.R. (mrosenfeld@ucsd.edu), R.G. (rgherzi@ucsd.edu) or A.R. (aramos@nimr.mrc.ac.uk).

METHODS

Identification of Dicer-interacting proteins. Anti-Dicer monoclonal antibodies 33, 73 and 83 and control monoclonal antibodies[11] were crosslinked to protein G–Sepharose 4 Fast Flow (Amersham Bioscience) and used to purify Dicer complexes from HEK293T (293T) cytoplasmic extracts (S10, ref. 11). Coimmunoprecipitates were washed five times with lysis buffer (20 mM Tris-HCl, pH 7.5, 300 mM NaCl, 0.5% NP-40, 2.5 mM $MgCl_2$). Proteins were separated by 10% SDS–PAGE. Protein-containing gel fragments were digested with trypsin as described previously[29] and analysed by liquid chromatography tandem mass spectrometry (LCQ Deca XP, Thermo 7 Finnigan). Proteins were identified using Turbo Sequest and MASCOT, searching the SwissProt database restricted to human proteins. A protein was considered as 'identified' if at least two peptides were in the first rank, concerning the correlation of experimental with theoretical data, with an ion score greater than 25. Peptides with ion scores of between 20 and 40 were peer-reviewed for their quality of alignment. No KSRP-specific peptides were identified in immunoprecipitations with isotype-control monoclonal antibodies.

NMR and circular dichroism spectroscopy. All circular dichroism spectra were recorded on a Jasco J-715 spectropolarimeter (Jasco) equipped with a PTC-348 Peltier temperature-control system. RNA binding was monitored by adding increasing amounts of protein to 2 μM *TL-let-7a-1* RNA in 10 mM Tris-HCl, pH 7.4, 100 mM NaCl, 0.5 mM TCEP. A temperature of 5 °C was chosen to optimize the signal change upon protein binding. The integral of the signal of between 255 nm and 265 nm was fitted against the protein concentration using in-house programs described previously[30] and the K_d values were extracted. All NMR spectra were recorded on Bruker Avance spectrometers operating at 600 and 700 MHz ^{1}H frequencies fitted with a supercooled probe. The spectra were processed with the NMRPipe package[31] and analysed with Sparky[32]. Solutions of 25 μM ^{15}N-labelled samples of KH3, KH4 and KH3–4 in 10 mM Tris-HCl buffer, 50 mM NaCl, 1 mM TCEP, pH 7.4, were titrated with *TL-let-7a-1* RNA oligonucleotides. ^{15}N-^{1}H HSQC spectra were recorded at each point of the titration at 27 °C. Amide chemical shift changes as a function of RNA/protein ratio were fitted to obtain the K_d values for the complexes using in-house software as described previously[30]. Weighted average values of ^{15}N and ^{1}H chemical shift variations have been calculated by $\Delta\delta_{av} = [(\Delta\delta^1\mathrm{H})^2 + (\Delta\delta^{15}\mathrm{N}/10)^2]^{1/2}$, and used to map *TL-let-7a-1* binding on a MolMol-generated molecular surface[33].

Preparation of RNA substrates and *in vitro* processing assays. For pri-miRNA processing assays, total cell extracts were prepared in 50 mM Tris-HCl, pH 8.0, 150 mM NaCl, 0.5% Triton X-100, 1× Complete, 10% glycerol from either HeLa or 293T cells and incubated (typically 40 μg per 25-μl reaction at 37 °C for the indicated times) with *in vitro* synthesized and uniformly labelled pri-miRNAs (5 fmol) in processing buffer containing 100 mM KCH_3COOH, 2 mM $Mg(CH_3COOH)_2$, 10 mM Tris-Cl, pH 7.6, 2 mM DTT, 10 mM creatine phosphate, 1 μg creatine phosphokinase, 1 mM ATP, 0.4 mM GTP, 0.1 mM spermine, 2 units of RNasin. Pre-miRNA processing assays were performed as described previously[11].

miRNA profiling. HeLa cells were transiently transfected with either siRNA against KSRP or siRNA against luciferase. Total RNA was prepared using Trizol (Invitrogen) and enriched with RNA smaller than 40 nucleotides using PureLink miRNA isolation kit. RNA was labelled with either Cy-3 or Cy-5 using the NCode miRNA labelling system. A dye-swap design was used. Labelled miRNAs were hybridized, in triplicate, to the Invitrogen NCode MultiSpecies miRNA Microarray V1. Data were collected using GenePixPro 5.0 Agilent Software (Axon Instruments). Normalization and data analysis were performed using a bootstrapping method[34].

Recombinant proteins and antibodies. Recombinant Dicer was purified as described previously[35]. MBP–TRBP was expressed in bacteria and purified as described previously[36]. Production of recombinant KSRP and its deletion mutants as well as p37AUF1 has been described previously[9]. Affinity-purified rabbit polyclonal anti-KSRP antibody, and rabbit polyclonal anti-Dicer (349), were described previously[9,37]. Mouse monoclonal anti-GST was purchased from Chemicon. Mouse monoclonal anti-Flag (M2) and anti-α- and -β-tubulin were from Sigma. Rabbit polyclonal anti-Drosha (07-717) was purchased from Upstate, anti-DGCR8 (N-19) goat polyclonal IgG from Santa Cruz and anti-Lin28 goat polyclonal IgG from R&D Systems.

Plasmids. Human *pre-let-7a-1* and *pre-miR-23b* were cloned into pSUPER-gfp-neo plasmid (Oligoengine). Chimaeric constructs including either the TL sequence of miR-23b in the backbone of *pre-let-7a-1* (UGAGGUAGUAGGUUGUAUAGUUGUGACUUAAGAUUAAACUAUACAAUCUACUGUCUUUC) or the TL sequence of let-7a-1 in the backbone of *pre-miR-23b* (UGGGUUCCUGGCAUGCUGAUUUUUAGGGUCACACCCACCACUGGGAGAUAAAUCACAUUGCCAGGGAUUACC) were generated and cloned into pSUPER-gfp-neo. pCY vector[38] containing part of the sequence (encompassing the mature miRNA) of either *pri-let-7a-1* or *pri-miR-23b* was generated. Three miR-23b-binding sites from a region between 360 and 385 nucleotides of semaphorin 6D 3′ untranslated region were cloned in pMIR-REPORT plasmid (Ambion). This sequence is a potential target of miR-23b according to TargetScan prediction program (http://www.targetscan.org). Flag–Dicer (provided by M. Doyle) and Flag–TRBP contain a triple Flag tag at the amino terminus of proteins expressed from the pCIneo vector (A.D.H., unpublished). Flag–KSRP was described previously[39]. A luciferase reporter gene plasmid containing six let-7a-binding sites and a plasmid containing genomic sequence encoding *pri-let-7a* were gifs from J. G. Belasco. Flag–Drosha and Flag–DGCR8 were provided by V. Narry Kim. Myc-tagged exportin-5 was provided by Addgene (Addgene plasmid number 12552). Part of the genomic sequence encompassing mouse *pre-miR-1-2* (*pri-miR-1-2*) was cloned into pcDNA3 vector (Invitrogen). Mouse *pre-miR-1-2* was cloned into pSUPER-gfp-neo plasmid (Oligoengine). A luciferase reporter gene plasmid containing four miR-1-binding sites was provided by D. Srivastava.

Cell transfection, coimmunoprecipitation and immunoblotting. HeLa, U2OS, P19 or NIH-3T3 cells were transiently transfected with Lipofectamine 2000 (Invitrogen). After either 48 h or 72 h, cells were collected, washed with PBS, resuspended in lysis buffer, and the protein concentration of cell extracts determined by the Dc Protein assay (Bio-Rad). When required, cell lysates were incubated at room temperature with either RNase A (10 μg ml^{-1}, Ambion) or RNase V1 (1 U ml^{-1}, Ambion) for 30 or 15 min, respectively. Three-hundred micrograms of protein was immunoprecipitated with protein A–Sepharose-bound anti-KSRP antibody for 16 h at 4 °C with rotation. Immunoprecipitates were washed four times with lysis buffer and resuspended in SDS protein loading buffer. Proteins were subjected to SDS–PAGE, electroblotted onto PVDF membranes, and probed with antibodies as indicated. Anti-connexin 43 antibody was from Sigma, anti-DNA pol α (G-16) was from Santa Cruz and anti-myogenin (F5D) was from Iowa Hybridoma Bank. C2C12 myoblasts were cultured and treated as described previously[40] and transfected using Lipofectamine 2000.

Northern blot analysis. RNA was extracted using Trizol, resolved on 15% polyacrylamide–urea gels, and electroblotted onto HyBond N$^+$ membranes. Membranes were hybridized overnight with radiolabelled antisense miRNAs in ExpressHyb solution (Clontech). After hybridization, membranes were washed three times with 2× SSC and 0.05% SDS, twice with 0.1× SSC and 0.1% SDS, exposed overnight to imaging screens, and analysed using a Storm 860 PhosphorImager. Signals were quantified using Imagequant V1.2. The same blot was hybridized (upon stripping in boiling 0.1% SDS) with three distinct probes, including control U6 RNA.

Luciferase assay. Either HeLa or NIH-3T3 cells (80% confluence in 12-well plates) were transfected with Luc reporters containing either six let-7a-binding sites (pGL3-let-7a6XBS) or three miR-23b-binding sites (pGL3-miR-23b3XBS), or empty pGL3 plasmid together with siRNAs using Lipofectamine 2000. For some experiments, cells were co-transfected with either *pri-let-7a-1* or *pre-let-7a-1* expression plasmids or mature let-7a. A co-transfected β-galactosidase-containing plasmid was used to normalize firefly luciferase activity.

EdU incorporation for proliferation assay. Seventy-two hours after transfection, cells were incubated for 2 h with EdU-containing medium. Nuclear incorporation of EdU was determined using Click-iT EdU imaging kit (Invitrogen).

Crystal violet proliferation assay. Seventy-two hours after transfection, U2OS cells were fixed and stained with crystal violet solution. After two washes with water, crystal violet staining was measured by spectrophotometer at a wavelength of 590 nm.

Tunel assay. Tunel-fluorescent staining of apoptotic cells was performed on U-2OS 72 h after the transfection according to the manufacturer's protocol (Roche).

Ultraviolet-crosslinking experiments and gel mobility shift assays. Ultraviolet-crosslinking experiments and gel mobility shift assays were performed essentially as described[9,38].

Expression and purification of the recombinant proteins used for biophysical studies. KSRP KH3, KH4 and KH3–4 proteins were obtained as described previously[10]. In brief, ^{15}N-labelled proteins were expressed in *Escherichia coli* BL21 (DE3), as His–GST fusion protein, and initially purified using nickel affinity chromatography according to the manufacturer's instructions. The His–GST fusion tags were then cleaved with TEV protease and removed using a second nickel affinity step. Proteins were further purified and buffer exchanged by gel filtration (Superdex 75 16/60 column, Pharmacia). Protein purity (always >95%) was assessed using SDS–PAGE and Coomassie blue staining. Protein quantification was achieved by a combination of spectrophotometry using predicted extinction coefficients and ninhydrin analysis of protein hydrolysates. All RNA oligonucleotides were chemically synthesized (Dharmacon).

shRNA-mediated KSRP knockdown. To knockdown stably KSRP, the following oligonucleatides 5′-GATCAACCGGAGAGCAAGA-3′ and 5′-GGACAG TTTCACGACAACG-3′ for human and mouse proteins, respectively, were

cloned into pSUPER-Puro (Oligoengine). 293T, NIH-3T3 or C2C12 cells were transfected using Lipofectamine Plus (Invitrogen). Transfectant pools were kept under selection in medium containing either 3 $\mu g\,ml^{-1}$ (293T) or 1.2 $\mu g\,ml^{-1}$ puromycin (NIH-3T3).

RT–PCR and quantitative PCR. PCR with reverse transcription (RT–PCR) and quantitative PCR were performed as described previously[41].

siRNAs. To knockdown the following human proteins, these siRNAs were synthesized by Qiagen: human KSRP 5′-GAUCAACCGGAGAGCAAGAUU-3′, mouse KSRP 5′-GGACAGUUUCACGACAACG-3′, mouse Lin28 5′-GGGUUGUGAUGACAGGCAA-3′, human Dicer 5′-GAAUCAGCCUCGCAACAAAUU-3′, luciferase 5′-CGUACGCGGAAUACUUCGAUU-3′.

29. Schrimpf, S. P., Langen, H., Gomes, A. V. & Wahlestedt, C. A two-dimensional protein map of Caenorhabditis elegans. *Electrophoresis* **22,** 1224–1232 (2001).
30. Martin, S. R. *et al.* Interaction of calmodulin with the phosphofructokinase target sequence. *FEBS Lett.* **577,** 284–288 (2004).
31. Delaglio, F. *et al.* NMRPipe: a multidimensional spectral processing system based on UNIX pipes. *J. Biomol. NMR* **6,** 277–293 (1995).
32. Goddard, T. D. & Kneller, D. G. *SPARKY, University of California, San Francisco* ⟨http://www.cgl.ucsf.edu/home/sparky/⟩.
33. Koradi, R., Billeter, M. & Wuthrich, K. MOLMOL: a program for display and analysis of macromolecular structures. *J. Mol. Graph.* **51-5,** 29–32 (1996).
34. Kerr, M. K. & Churchill, G. A. Experimental design for gene expression microarrays. *Biostatistics* **2,** 183–201 (2001).
35. Zhang, H., Kolb, F. A., Brondani, V., Billy, E. & Filipowicz, W. Human Dicer preferentially cleaves dsRNAs at their termini without a requirement for ATP. *EMBO J.* **21,** 5875–5885 (2002).
36. Dorin, D. *et al.* The TAR RNA-binding protein, TRBP, stimulates the expression of TAR-containing RNAs in vitro and in vivo independently of its ability to inhibit the dsRNA-dependent kinase PKR. *J. Biol. Chem.* **278,** 4440–4448 (2003).
37. Kotaja, N. *et al.* The chromatoid body of male germ cells: similarity with processing bodies and presence of Dicer and microRNA pathway components. *Proc. Natl Acad. Sci. USA* **103,** 2647–2652 (2006).
38. Chen, C. Y. *et al.* AU binding proteins recruit the exosome to degrade ARE-containing mRNAs. *Cell* **107,** 451–464 (2001).
39. Briata, P. *et al.* p38-dependent phosphorylation of the mRNA decay-promoting factor KSRP controls the stability of select myogenic transcripts. *Mol. Cell* **20,** 891–903 (2005).
40. Wu, Z. *et al.* p38 and extracellular signal-regulated kinases regulate the myogenic program at multiple steps. *Mol. Cell. Biol.* **20,** 3951–3964 (2000).
41. Gherzi, R. *et al.* The RNA-binding protein KSRP promotes decay of beta-catenin mRNA and is inactivated by PI3K-AKT signaling. *PLoS Biol.* **5,** e5 (2006).